Available online at www.sciencedirect.com
SCIENCE DIRECT®
Journal of Sound and Vibration 280 (2005) 633–655
JOURNAL OF SOUND AND VIBRATION
www.elsevier.com/locate/jsvi

Free vibration analysis of stepped circular Mindlin plates

Y. Xiang[a,b,*], L. Zhang[b]

[a] School of Engineering and Industrial Design, University of Western Sydney, Penrith South DC, NSW 1797, Australia
[b] Centre for Construction Technology and Research, University of Western Sydney, Penrith South DC, NSW 1797, Australia

Received 17 January 2003; accepted 12 December 2003

Abstract

This paper presents the first-known investigation on exact vibration of circular Mindlin plates with multiple step-wise thickness variations. A stepped circular plate is divided into multiple annular and one circular segments along the locations of the step variations. The governing differential equations for harmonic vibration of annual and circular segments are derived and an analytical method based on the domain decomposition technique is developed to solve the plate vibration problem. Exact vibration solutions are presented for circular Mindlin plates of different edge support conditions and various combinations of step-wise thickness variations. The influence of plate boundary conditions, plate thickness ratios, step location ratios and step thickness ratios on the vibration behaviour of stepped circular Mindlin plates are examined. The exact vibration results can serve as benchmark values for researchers to validate their numerical methods for such circular plate problems.

1. Introduction

Circular plates with non-uniform thickness variations have wide practical applications in civil, mechanical and aerospace engineering due to the potential savings on material usage and/or weight reduction of the plates. Extensive studies have been carried out for the vibration of circular plates in various forms of thickness variations. Many of the studies have been well documented in the excellent reviews of Leissa [1–7] and other publications [8–10].

The vibration of circular and annular plates with non-linear thickness variations has been studied by Lee and Ng [11], Wang [12], Chen and Ren [13], Singh and Hassan [14], Gupta and Sharma [15], Ye [16], Wu and Liu [17], and Gajewski [18]. More studies have been carried out on

*Corresponding author. Tel.: +61-2-4736-0395; fax: +61-2-4736-0833.
E-mail address: y.xiang@uws.edu.au (Y. Xiang).

0022-460X/$ - see front matter © 2003 Elsevier Ltd. All rights reserved.
doi:10.1016/j.jsv.2003.12.017

the vibration of circular and annular plates with tapered (linear) thickness variations [8–10,12,17,19–23]. Vibration of circular plates with step-wise thickness variations is another important area that has been studied by many researchers [24–28]. Different plate theories have been applied in studying the vibration of circular and annular plates with variable thickness, ranging from the classical thin plate theory [12,17], to the shear deformable plate theory [19] to 3-D elasticity theory [8]. The Rayleigh–Ritz method is one of the most popular methods that have been used to study the vibration of circular plates with thickness variations [8–10]. Other methods that are used in this area include the finite element method [13], analytical method [12] and differential quadrature method [17], etc.

To the authors' best knowledge, there are no exact solutions available in open literature for vibration of circular Mindlin plates with stepped thickness variations. The primary objective of this paper is to present exact vibration frequencies for stepped circular Mindlin plates. An analytical method proposed by the first author [29] for vibration of circular Mindlin plates with ring supports is modified to study the vibration behaviour of stepped circular Mindlin plates. Comparison studies are carried out to verify the correctness of the proposed method. Extensive exact vibration frequencies and modal shapes are presented for circular Mindlin plates with different edge support conditions and various combinations of step configurations. The influence of the plate thickness ratios, step thickness ratios and step locations on the vibration behaviour of circular Mindlin plates is highlighted in the paper.

2. Mathematical modelling

Consider an isotropic, elastic circular plate of radius R as shown in Fig. 1. The plate consists of m steps with radii $r_1(=R), r_2, \ldots, r_m$, and step thicknesses $h_1, h_2, \ldots, h_m$, respectively. The plate is of Young's modulus E, shear modulus $G = E/[2(1+\nu)]$, mass density ρ and ν is the Poisson ratio. The plate may have free, simply supported or clamped edge support conditions. The problem at hand is to determine the natural frequencies of the stepped circular plate. The Mindlin first order shear deformable plate theory [30] is employed to study this problem.

The vibration of circular Mindlin plates with concentric ring supports has been studied by the first author [29] recently and the analytical approach in Ref. [29] is extended in this paper to study the vibration of circular Mindlin plates with multiple step variations. The circular plate is first divided into several annular segments and one circular segment along the locations of the step variations. Using the polar co-ordinate system shown in Fig. 1, the equations of motion for the ith segment may be expressed as [31,32]:

$$\begin{aligned}
&\frac{\partial}{\partial r}\left\{D_i\left[\frac{\partial \psi_r^i}{\partial r}+\frac{\nu}{r}\left(\psi_r^i+\frac{\partial \psi_\theta^i}{\partial \theta}\right)\right]\right\}+\frac{1}{r}\frac{\partial}{\partial \theta}\left\{\frac{(1-\nu)D_i}{2}\left[\frac{1}{r}\left(\frac{\partial \psi_i^r}{\partial \theta}-\psi_\theta^i\right)+\frac{\partial \psi_\theta^i}{\partial r}\right]\right\}\\
&\quad+\frac{1}{r}\left\{D_i\left[\frac{\partial \psi_r^i}{\partial r}+\frac{\nu}{r}\left(\psi_r^i+\frac{\partial \psi_\theta^i}{\partial \theta}\right)\right]-D_i\left[\frac{1}{r}\left(\psi_r^i+\frac{\partial \psi_\theta^i}{\partial \theta}\right)+\nu\frac{\partial \psi_r^i}{\partial r}\right]\right\}\\
&\quad-\kappa^2 G h_i\left(\psi_r^i+\frac{\partial w^i}{\partial r}\right)+\frac{\rho h_i^3\omega^2}{12}\psi_r^i=0,
\end{aligned} \tag{1}$$

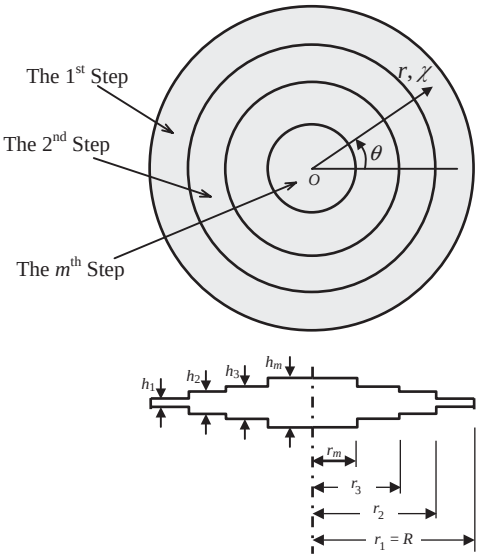

Fig. 1. Geometry and co-ordinate system for a stepped circular plate.

$$\frac{\partial}{\partial r}\left\{D_i\left[\frac{\partial\psi_r^i}{\partial r}+\frac{v}{r}\left(\psi_r^i+\frac{\partial\psi_\theta^i}{\partial\theta}\right)\right]\right\}+\frac{1}{r}\frac{\partial}{\partial\theta}\left\{\frac{(1-v)D_i}{2}\left[\frac{1}{r}\left(\frac{\partial\psi_i^r}{\partial\theta}-\psi_\theta^i\right)+\frac{\partial\psi_\theta^i}{\partial r}\right]\right\}$$
$$+\frac{1}{r}\left\{D_i\left[\frac{\partial\psi_r^i}{\partial r}+\frac{v}{r}\left(\psi_r^i+\frac{\partial\psi_\theta^i}{\partial\theta}\right)\right]-D_i\left[\frac{1}{r}\left(\psi_r^i+\frac{\partial\psi_\theta^i}{\partial\theta}\right)+v\frac{\partial\psi_r^i}{\partial r}\right]\right\}$$
$$-\kappa^2 Gh_i\left(\psi_r^i+\frac{\partial w^i}{\partial r}\right)+\frac{\rho h_i^3\omega^2}{12}\psi_r^i=0, \tag{2}$$

$$\frac{1}{r}\frac{\partial}{\partial r}\left[\kappa^2 Gh_i\left(\psi_r^i+\frac{\partial w^i}{\partial r}\right)r\right]+\frac{1}{r}\frac{\partial}{\partial\theta}\left[\kappa^2 Gh_i\left(\psi_\theta^i+\frac{1}{r}\frac{\partial w^i}{\partial\theta}\right)\right]+\rho h_i\omega^2 w^i=0, \tag{3}$$

in which w^i, ψ_r^i and ψ_θ^i are the transverse deflection and the rotations in the θ and r directions at the midsurface of the plate, respectively, r and θ are the radial and circumferential co-ordinates, $D_i = Eh_i^3/[12(1-v^2)]$ is the flexural rigidity of the plate, κ^2 is the shear correction factor required in the Mindlin plate theory, and ω is the circular frequency.

The displacement fields of the ith segment may be expressed as functions of three potentials Θ_1^i, Θ_2^i and Θ_3^i:

$$\psi_r^i=[(\sigma_1)_i-1]\frac{\partial\Theta_1^i}{\partial\chi}+[(\sigma_2)_i-1]\frac{\partial\Theta_2^i}{\partial\chi}+\frac{1}{\chi}\frac{\partial\Theta_3^i}{\partial\theta}, \tag{4}$$

$$\psi_\theta^i=[(\sigma_1)_i-1]\frac{1}{\chi}\frac{\partial\Theta_1^i}{\partial\theta}+[(\sigma_2)_i-1]\frac{1}{\chi}\frac{\partial\Theta_2^i}{\partial\theta}-\frac{\partial\Theta_3^i}{\partial\chi}, \tag{5}$$

$$\bar{w}^i=\Theta_1^i+\Theta_2^i, \tag{6}$$

where

$$(\sigma_1)_i, (\sigma_2)_i = \frac{2((\delta_2^2)_i, (\delta_1^2)_i)}{(\delta_3^2)_i(1-\nu)}, \tag{7}$$

$$(\delta_1^2)_i, (\delta_2^2)_i = \frac{\lambda_i^2}{2}\left[\frac{\tau_i^2}{12} + \frac{\tau_i^2}{6(1-\nu)\kappa^2} \pm \sqrt{\left(\left(\frac{\tau_i^2}{12} - \frac{\tau_i^2}{6(1-\nu)\kappa^2}\right)^2 + \frac{4}{\lambda_i^2}\right)}\right], \tag{8}$$

$$(\delta_3^2)_i = \frac{2}{(1-\nu)}\left[\frac{\tau_i^2\lambda_i^2}{12} - \frac{6(1-\nu)^2}{\tau_i^2}\right], \tag{9}$$

$$\bar{w}^i = \frac{w^i}{R}, \quad \chi = \frac{r}{R}, \quad \tau_i = \frac{h_i}{R}, \quad \lambda_i = \omega R^2\sqrt{\frac{\rho h_i}{D_i}}. \tag{10}$$

$\bar{w}^i$ is the non-dimensionalized deflection of the plate, χ is the non-dimensionalized radial co-ordinate, and λ_i is the frequency parameter corresponding to the ith segment.

Based on the three potentials, the governing differential equations in Eqs. (1)–(3) may be transformed as

$$[\nabla^2 + (\delta_1^2)_i]\Theta_1^i = 0, \tag{11}$$

$$[\nabla^2 + (\delta_2^2)_i]\Theta_2^i = 0, \tag{12}$$

$$[\nabla^2 + (\delta_3^2)_i]\Theta_3^i = 0, \tag{13}$$

where the Laplacian operator in polar co-ordinates is given by

$$\nabla^2(\cdot) = \frac{\partial^2(\cdot)}{\partial\chi^2} + \frac{1}{\chi}\frac{\partial(\cdot)}{\partial\chi} + \frac{1}{\chi^2}\frac{\partial^2(\cdot)}{\partial\theta^2}. \tag{14}$$

The solutions to Eqs. (11)–(13) for the ith segment can be derived as [31,32]

$$\Theta_1^i = A_1^i R_n(\Delta_1^i\chi)\cos n\theta + B_1^i S_n(\Delta_1^i\chi)\cos n\theta, \tag{15}$$

$$\Theta_2^i = A_2^i R_n(\Delta_2^i\chi)\cos n\theta + B_2^i S_n(\Delta_2^i\chi)\cos n\theta, \tag{16}$$

$$\Theta_3^i = A_3^i R_n(\Delta_3^i\chi)\sin n\theta + B_3^i S_n(\Delta_3^i\chi)\sin n\theta, \tag{17}$$

where $n = (1, 2, \ldots, \infty)$ is the number of nodal diameters of a vibration mode, A_j^i and B_j^i, $j = 1, 2$ and 3, are the arbitrary constants that will be determined by the boundary conditions and interface continuity conditions between segments, and

$$\Delta_j^i = \begin{cases} (\delta_j)_i & \text{if } (\delta_j^2)_i \geqslant 0, \\ \mathrm{Im}(\delta_j)_i & \text{if } (\delta_j^2)_i < 0, \end{cases} \quad j = 1, 2, 3, \tag{18}$$

$$R_n(\Delta_j^i\chi) = \begin{cases} \mathrm{J}_n(\Delta_j^i\chi) & \text{if } (\delta_j^2)_i \geqslant 0, \\ \mathrm{I}_n(\Delta_j^i\chi) & \text{if } (\delta_j^2)_i < 0, \end{cases} \quad j = 1, 2, 3, \tag{19}$$

$$S_n(\Delta_j^i\chi) = \begin{cases} \mathrm{Y}_n(\Delta_j^i\chi) & \text{if } (\delta_j^2)_i \geqslant 0, \\ \mathrm{K}_n(\Delta_j^i\chi) & \text{if } (\delta_j^2)_i < 0, \end{cases} \quad j = 1, 2, 3, \tag{20}$$

in which $\mathrm{J}_n(\cdot)$ and $\mathrm{Y}_n(\cdot)$ are Bessel functions of the first kind and the second kind of order n, respectively, and $\mathrm{I}_n(\cdot)$ and $\mathrm{K}_n(\cdot)$ are the modified Bessel functions of the first kind and the second kind of order n, respectively. Note that for the circular segment ($i = m$), the arbitrary constants B_j^i must be set to zero to prevent singularity for the displacement fields w^i, ψ_r^i and ψ_θ^i at the plate centre ($\chi = r/R = 0$).

The boundary conditions of a circular Mindlin plate can be expressed as

$$M_{rr}^i = M_{r\theta}^i = Q_r^i = 0, \quad \text{for free edge,} \tag{21}$$

$$M_{rr}^i = \psi_0^i = \bar{w}^i = 0, \quad \text{for simply supported edge,} \tag{22}$$

$$\psi_r^i = \psi_\theta^i = \bar{w}^i = 0, \quad \text{for clamped edge,} \tag{23}$$

where the stress resultants for shear force and bending moments Q_r^i, M_{rr}^i and $M_{r\theta}^i$ are given by [33]

$$Q_r^i = \kappa^2 G h_i \left(\frac{\partial \bar{w}^i}{\partial \chi} + \psi_r^i \right), \tag{24}$$

$$M_{rr}^i = \frac{D_i}{R} \left[\frac{\partial \psi_r^i}{\partial \chi} + \frac{\nu}{\chi} \left(\psi_r^i + \frac{\partial \psi_\theta^i}{\partial \theta} \right) \right]. \tag{25}$$

$$M_{r\theta}^i = \frac{D_i}{R} \left(\frac{1-\nu}{2} \right) \left[\frac{1}{\chi} \left(\frac{\partial \psi_r^i}{\partial \theta} - \psi_\theta^i \right) + \frac{\partial \psi_\theta^i}{\partial \chi} \right]. \tag{26}$$

To satisfy the thickness variation and ensure the continuity along the interface of the ith and $(i+1)$th segments, the essential and natural interface conditions between the two segments must hold as follows:

$$\bar{w}^i = \bar{w}^{i+1}, \tag{27}$$

$$\psi_r^i = \psi_r^{i+1}, \tag{28}$$

$$\psi_\theta^i = \psi_\theta^{i+1}, \tag{29}$$

$$Q_r^i = Q_r^{i+1}, \tag{30}$$

$$M_{rr}^i = M_{rr}^{i+1}, \tag{31}$$

$$M_{r\theta}^i = M_{r\theta}^{i+1}. \tag{32}$$

The displacement fields and stress resultants of the ith segment can be expressed in terms of the arbitrary constants A_j^i and B_j^i, $j = 1, 2$ and 3, as detailed in Ref. [29]. In view of Eqs. (4)–(6) and (15)–(17) and implementing the boundary conditions of the plate along the circumferential edge and interface conditions between segments, a homogeneous system of equations for the stepped

circular Mindlin plate can be derived as

$$\mathbf{K}[\mathbf{A}^1\ \mathbf{B}^1 \cdots \mathbf{A}^i\ \mathbf{B}^i \cdots \mathbf{A}^{m-1}\ \mathbf{B}^{m-1}\ \mathbf{A}^m]^{\mathrm{T}} = \{0\}, \tag{33}$$

in which

$$\mathbf{A}^i = [A_1^i\ A_2^i\ A_2^i], \tag{34}$$

$$\mathbf{B}^i = [B_1^i\ B_2^i\ B_2^i], \tag{35}$$

m is the number of segments of the circular plate, and $\mathbf{K}$ is a $(6m-3)\times(6m-3)$ matrix. The angular frequency ω of the plate is evaluated by setting the determinant of $\mathbf{K}$ in Eq. (33) to be zero.

Matlab is employed in this study to compute the eigenvalues and eigenvectors as governed by Eq. (33). An eigenvalue ω is determined when the determinant of matrix $\mathbf{K}$ in Eq. (33) is equal to 0. In the search for the eigenvalue, an iterative process is developed. Firstly, we set an initial value for ω and small increments of ω are subsequently added to the initial value. The determinants of $\mathbf{K}$ are evaluated accordingly. Once the sign of the determinant $\mathbf{K}$ changes, an eigenvalue of ω exists in between the two previous increments of ω. The bisection method is then utilized to find the eigenvalue. In the bisection search, the calculation stops when a given tolerance between the two successive values of ω is reached. In this study, the tolerance is set to be $|(\omega_i-\omega_{i-1})/\omega_i| \leqslant 1/10\,000\,000\,000$.

3. Results and discussions

The proposed analytical method may be used to obtain exact vibration frequencies for circular Mindlin plates of arbitrary number of step variations. In this section, the analytical method is

Table 1
Comparison study of frequency parameters $\lambda = \omega R^2\sqrt{\rho h_1/D_1}$ for circular Mindlin plates with one step variation ($h_1/R = 0.005, r_2/R = 0.5$)

Boundary conditions	h_2/h_1	Sources	Mode sequence				
			1	2	3	4	5
Simply supported	1	Avalos et al. [25]	4.93515	29.7200	74.1561	138.318	222.215
	1	Present	4.93504	29.7160	74.1308	138.230	221.988
	1.5	Avalos et al. [25]	5.82394	35.0578	89.6624	169.730	269.625
	1.5	Present	5.75819	35.0577	88.0734	169.103	264.323
	2	Avalos et al. [25]	6.25945	41.4173	99.4271	200.067	306.328
	2	Present	6.03078	41.3104	95.1796	194.462	297.972
Clamped	1	Avalos et al. [25]	10.2158	39.7711	89.1042	158.184	247.006
	1	Present	10.2151	39.7617	89.0601	158.051	246.090
	1.5	Avalos et al. [25]	11.1450	46.5721	109.520	191.761	302.675
	1.5	Present	11.0856	46.3787	107.695	191.126	295.822
	2	Avalos et al. [25]	11.8799	53.7887	122.863	226.337	342.540
	2	Present	11.5842	53.6290	116.659	222.965	327.017

Table 2
Frequency parameters $\lambda = \omega R^2\sqrt{\rho h_1/D_1}$ for circular Mindlin plates with one step variation ($h_1/R = 0.005, r_2/R = 0.5$)

Boundary conditions	h_2/h_1	Mode sequence									
		1	2	3	4	5	6	7	8	9	10
Free	0.5	4.41721(2,1)	6.80950(0,1)	11.5610(3,1)	15.2987(1,1)	21.1649(4,1)	25.1370(0,2)	28.8731(2,2)	33.0297(5,1)	43.1093(1,2)	45.4902(3,2)
	1.5	7.05244(2,1)	11.6881(0,1)	13.9314(3,1)	22.8594(4,1)	23.3520(1,1)	34.1194(5,1)	38.9967(2,2)	44.7776(0,2)	47.7163(6,1)	59.0696(3,2)
	2	8.94458(2,1)	13.4603(0,1)	15.4172(3,1)	23.8068(4,1)	24.0510(1,1)	34.6875(5,1)	42.2000(2,2)	48.0455(6,1)	51.7387(0,2)	63.7836(7,1)
Simply supported	0.5	4.03407(0,1)	11.1005(1,1)	21.4086(0,2)	21.9320(2,1)	35.4884(3,1)	37.0915(1,2)	52.1210(4,1)	53.2231(0,3)	54.4418(2,2)	69.6081(1,3)
	1.5	5.75819(0,1)	14.9431(1,1)	28.4443(2,1)	35.0577(0,2)	44.7828(3,1)	58.7990(1,2)	62.3004(4,1)	81.1281(5,1)	81.4831(2,2)	88.0734(0,3)
	2	6.03078(0,1)	14.9276(1,1)	31.8110(2,1)	41.3105(0,2)	50.5671(3,1)	65.7792(1,2)	67.9513(4,1)	85.6166(5,1)	86.6408(2,2)	95.1796(0,3)
Clamped	0.5	10.1734(0,1)	17.6859(1,1)	26.7448(0,2)	29.2213(2,1)	43.7493(1,2)	43.9983(3,1)	62.0158(4,1)	63.2399(2,2)	65.7056(0,3)	83.3649(5,1)
	1.5	11.0856(0,1)	23.2698(1,1)	38.5196(2,1)	46.3787(0,2)	57.2980(3,1)	74.0188(1,2)	77.4404(4,1)	98.3399(5,1)	100.533(2,2)	107.695(0,3)
	2	11.5842(0,1)	23.4381(1,1)	41.9606(2,1)	53.6290(0,2)	64.7335(3,1)	85.2313(1,2)	85.8569(4,1)	105.540(5,1)	108.821(2,2)	116.659(0,3)

The values in brackets (n, s) denote the number of nodal diameters (n) and the mode sequence (s) for a given n value

Table 3
Frequency parameters $\lambda = \omega R^2\sqrt{\rho h_1/D_1}$ for circular Mindlin plates with one step variation ($h_1/R = 0.10$, $r_2/R = 0.5$)

Boundary conditions	h_2/h_1	Mode sequence									
		1	2	3	4	5	6	7	8	9	10
Free	0.5	4.32805(2,1)	6.73006(0,1)	11.2017(3,1)	14.6336(1,1)	20.1792(4,1)	24.3612(0,2)	27.0789(2,2)	30.8834(5,1)	40.9033(1,2)	41.8569(3,2)
	1.5	6.88138(2,1)	11.4342(0,1)	13.3881(3,1)	21.6542(4,1)	22.2602(1,1)	31.7725(5,1)	36.1061(2,2)	41.0624(0,2)	43.5479(6,1)	52.7997(3,2)
	2	8.56567(2,1)	13.0908(0,1)	14.5691(3,1)	22.3198(4,1)	22.7786(1,1)	32.1222(5,1)	38.4314(2,2)	43.7244(6,1)	46.0270(0,2)	56.8297(7,1)
Simply supported	0.5	4.01011(0,1)	10.7583(1,1)	20.8502(0,2)	21.0157(2,1)	33.4553(3,1)	35.3408(1,2)	47.9946(4,1)	49.7370(0,3)	50.3917(2,2)	63.8692(1,3)
	1.5	5.68854(0,1)	14.4923(1,1)	26.9433(2,1)	32.6687(0,2)	41.1944(3,1)	52.2897(1,2)	55.8052(4,1)	70.1948(5,1)	70.9304(2,2)	75.1929(0,3)
	2	5.94088(0,1)	14.3961(1,1)	29.5769(2,1)	37.4877(0,2)	45.1643(3,1)	56.8833(1,2)	59.2701(4,1)	73.0426(5,1)	73.4061(2,2)	78.9800(0,3)
Clamped	0.5	9.97265(0,1)	16.9103(1,1)	25.6426(0,2)	27.2909(2,1)	40.1942(3,1)	40.9660(1,2)	55.1754(4,1)	57.3216(2,2)	59.2026(0,3)	71.8933(5,1)
	1.5	10.6655(0,1)	21.7095(1,1)	35.0502(2,1)	41.5770(0,2)	50.3801(3,1)	62.7243(1,2)	65.7979(4,1)	81.1364(5,1)	81.5327(2,2)	86.5788(0,3)
	2	11.0254(0,1)	21.6130(1,1)	37.5335(2,1)	46.7177(0,2)	55.0429(3,1)	69.1943(1,2)	70.3428(4,1)	84.5375(5,1)	85.5328(2,2)	90.7940(0,3)

The values in brackets (n, s) denote the number of nodal diameters (n) and the mode sequence (s) for a given n value

Table 4
Frequency parameters $\lambda = \omega R^2\sqrt{\rho h_1/D_1}$ for circular Mindlin plates with one step variation ($h_1/R = 0.20, r_2/R = 0.5$)

Boundary conditions	h_2/h_1	Mode sequence									
		1	2	3	4	5	6	7	8	9	10
Free	0.5	4.17076(2,1)	6.51030(0,1)	10.4953(3,1)	13.4736(1,1)	18.2660(4,1)	22.4421(0,2)	23.9487(2,2)	26.9505(5,1)	35.5816(3,2)	36.0800(1,2)
	1.5	6.58176(2,1)	10.7803(0,1)	12.4220(3,1)	19.4733(4,1)	19.9406(1,1)	27.6262(5,1)	30.7099(2,2)	34.2397(0,2)	36.5790(6,1)	42.6805(3,2)
	2	7.99304(2,1)	12.1688(0,1)	13.2827(3,1)	19.8984(4,1)	20.1667(1,1)	27.8244(5,1)	31.9374(2,2)	36.6692(6,1)	36.8436(0,2)	44.9157(3,2)
Simply supported	0.5	3.94131(0,1)	10.1483(1,1)	19.1427(2,1)	19.4310(0,2)	29.2817(3,1)	31.4957(1,2)	40.2368(4,1)	42.7464(0,3)	43.0378(2,2)	51.7083(5,1)
	1.5	5.49567(0,1)	13.4062(1,1)	23.7328(2,1)	27.9355(0,2)	34.5948(3,1)	41.6326(1,2)	45.1069(4,1)	53.6708(2,2)	55.5166(5,1)	56.8614(0,3)
	2	5.69548(0,1)	13.1470(1,1)	25.3802(2,1)	30.7653(0,2)	36.8072(3,1)	43.6093(1,2)	46.8562(4,1)	54.3418(2,2)	56.6689(5,1)	58.0142(0,3)
Clamped	0.5	9.43854(0,1)	15.3759(1,1)	23.0564(0,2)	23.7311(2,1)	33.4375(3,1)	35.0708(1,2)	43.9764(4,1)	46.6404(2,2)	47.4725(0,3)	55.0560(5,1)
	1.5	9.65263(0,1)	18.5003(1,1)	28.7187(2,1)	33.3374(0,2)	39.4904(3,1)	46.8654(1,2)	49.6923(4,1)	58.3464(2,2)	59.5845(5,1)	61.3655(0,3)
	2	9.74498(0,1)	17.9919(1,1)	30.0974(2,1)	36.1946(0,2)	41.8725(3,1)	49.4751(1,2)	51.7344(4,1)	59.3872(2,2)	60.9587(5,1)	62.5477(0,3)

The values in brackets (n, s) denote the number of nodal diameters (n) and the mode sequence (s) for a given n value

applied to study the vibration behaviour of several selected stepped circular Mindlin plates. The Poisson ratio $v = 0.3$ and the shear correction factor $\kappa^2 = \frac{5}{6}$ are used in all calculations. The circular frequency ω is expressed in terms of a non-dimensional frequency parameter $\lambda = \omega R^2\sqrt{\rho h_1/D_1}$, where h_1 is the thickness of the first step and $D_1 = Eh_1^3/[12(1-v^2)]$.

3.1. Verification of solution method

Table 1 shows the frequency parameters λ obtained by the present solution approach and the Rayleigh–Ritz method [25] for circular plates with one step variation. The plate thickness ratio h_1/R is set to be 0.005 in order to compare the present results based on the Mindlin plate theory with the results from Avalos et al. [25] based on the thin plate theory. Note that the results from Avalos et al. [25] are for axisymmetric cases ($n = 0$). The number of terms of the polynomial employed in Ref. [25] is 10. It is observed that the first two frequency parameters λ from the present study are in good agreement with the ones from Avalos et al. [25]. Table 1 also shows that the frequency parameters λ for higher modes from Avalos et al. [25] are not quite yet converged to the present exact solutions. This comparison study confirms the correctness of the proposed analytical method.

3.2. Circular plates with one step variation

Tables 2–4 show the exact frequency parameters of the first 10 modes for free, simply supported and clamped circular Mindlin plates with one step variation. The location of the step variation is at $r_2/R = 0.5$ and the plate thickness ratio h_1/R is set to be 0.005, 0.1 and 0.2. Three step thickness ratios are considered, i.e., $h_2/h_1 = 0.5$, 1.5 and 2, respectively. As expected, frequency parameters λ increase as the step thickness ratio h_2/h_1 increases. The fundamental vibration mode for all simply supported and clamped plates in Tables 2–4 is axisymmetric ($n = 0$). The fundamental mode for all free plates, however, is not axisymmetric, where two nodal diameters ($n = 2$) exist in the fundamental vibration mode. The frequency parameters λ decrease as the plate thickness ratio h_1/R increases due to the effect of transverse shear deformation and rotary inertia.

The exact vibration solutions in Tables 2–4 are highly valuable as benchmark values to check the validity and accuracy of approximate numerical methods for the vibration of stepped circular plates. However, these results are not sufficient to show the effect of the step location ratio r_2/R, step thickness ratio h_2/h_1 and plate thickness ratio h_1/R on the vibration behaviour of stepped circular Mindlin plates. Figs. 2–6 are depicted to show the relationship between the frequency parameters λ and the step location ratio r_2/R, step thickness ratio h_2/h_1 and plate thickness ratio h_1/R for circular Mindlin plates with one step variation.

Figs. 2–4 present the variation of the first four frequency parameters λ versus the step location ratio r_2/R for free, simply supported and clamped circular Mindlin plates with one step variation. The step thickness ratio is fixed to be $h_2/h_1 = 2.0$ and the plate thickness ratio h_1/R varies from 0.005 to 1.0 to 2.0, respectively. The curves in Figs. 2–4 start from $r_2/R = 0.01$ and end at $r_2/R = 0.99$ and there are 99 sample points on each curve. Fig. 2 shows that the frequency parameters for free circular plates increase first and then decrease as the step location ratio r_2/R varies from 0.01 to 0.99. The optimal step thickness ratio for maximizing the frequency parameters of free circular plates is in the range of $r_2/R = 0.8$–0.9. The variation of the frequency

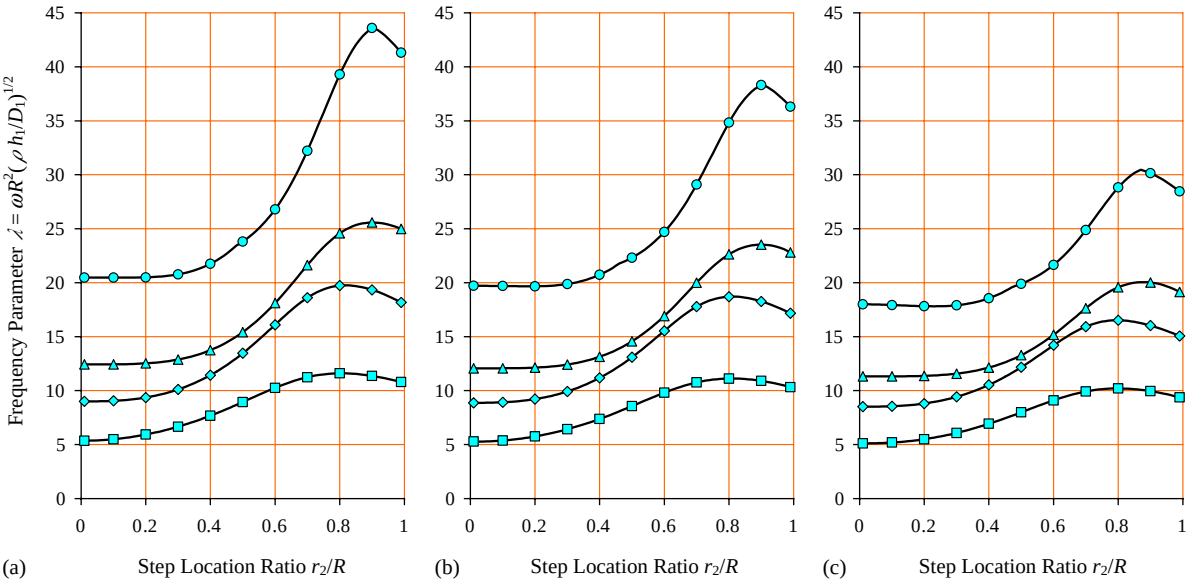

Fig. 2. Frequency parameters $\lambda = \omega R^2(\rho h_1/D_1)^{1/2}$ versus step location ratio r_2/R for free circular Mindlin plates having one step variation, step thickness ratio $h_2/h_1 = 2.0$ and plate thickness ratios $h_1/R =$ (a) 0.005, (b) 0.10 and (c) 0.20. □, First mode; ◇; second mode; △, third mode; and ○, fourth mode.

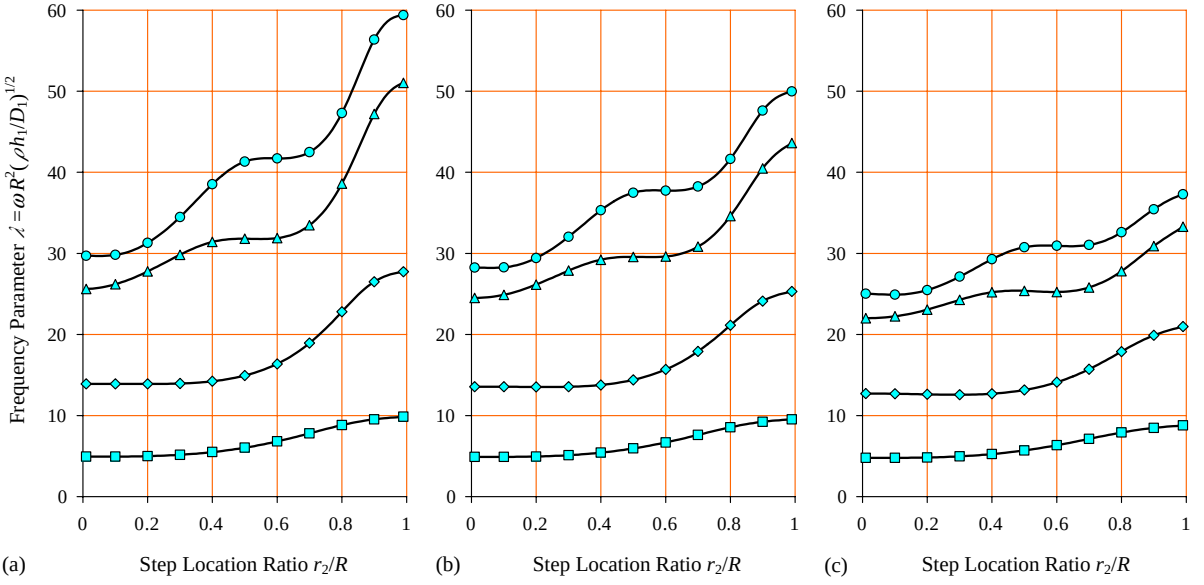

Fig. 3. Frequency parameters $\lambda = \omega R^2(\rho h_1/D_1)^{1/2}$ versus step location ratio r_2/R for simply supported circular Mindlin plates having one step variation, step thickness ratio $h_2/h_1 = 2.0$ and plate thickness ratios $h_1/R =$ (a) 0.005, (b) 0.10 and (c) 0.20. □, First mode; ◇, second mode; △, third mode; and ○, fourth mode.

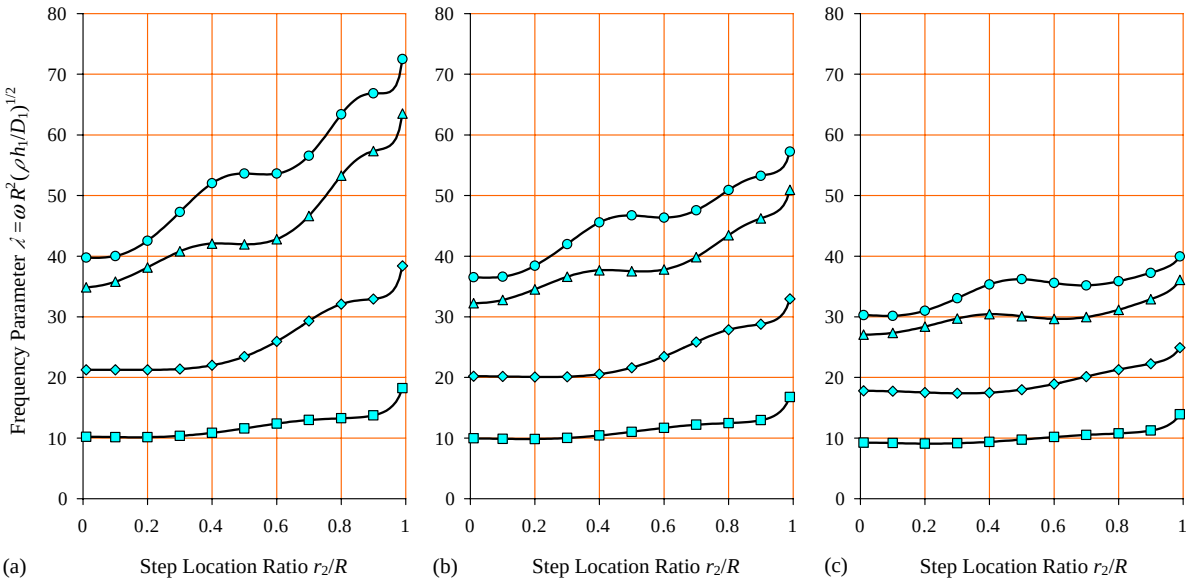

Fig. 4. Frequency parameters $\lambda = \omega R^2(\rho h_1/D_1)^{1/2}$ versus step location ratio r_2/R for clamped circular Mindlin plates having one step variation, step thickness ratio $h_2/h_1 = 2.0$ and plate thickness ratios $h_1/R =$ (a) 0.005, (b) 0.10 and (c) 0.20. □, First mode; ◇, second mode; △, third mode; and ○, fourth mode.

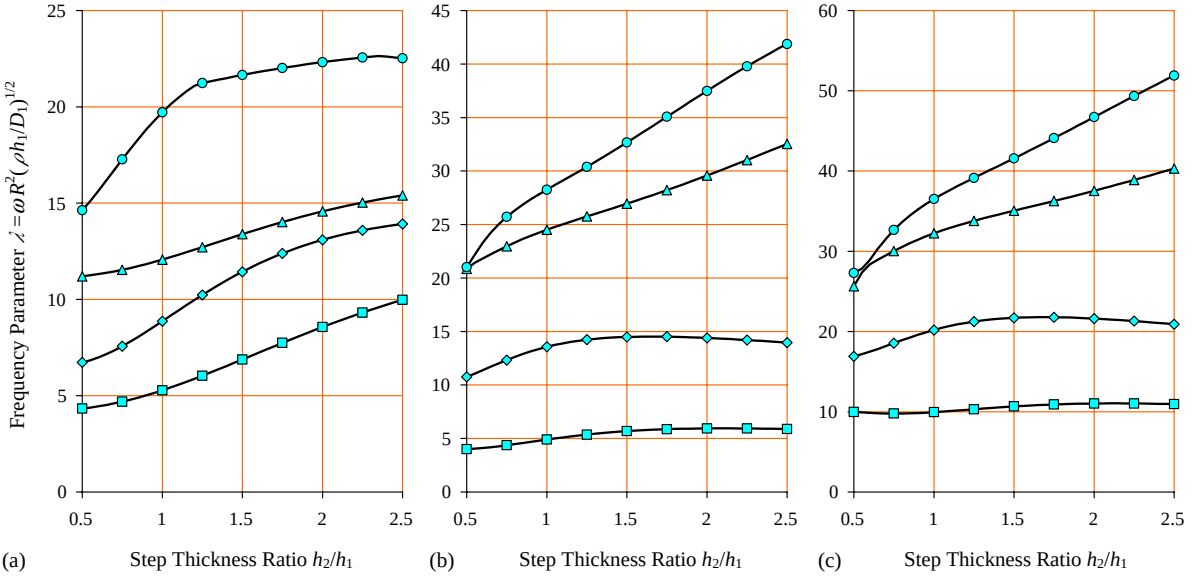

Fig. 5. Frequency parameters $\lambda = \omega R^2(\rho h_1/D_1)^{1/2}$ versus step thickness ratio h_2/h_1 for circular Mindlin plates (a) free, (b) simply supported, (c) clamped, having one step variation, step location ratio $r_2/R = 0.5$ and plate thickness ratios $h_1/R = 0.10$. □, First mode; ◇, second mode; △, third mode; and ○, fourth mode.

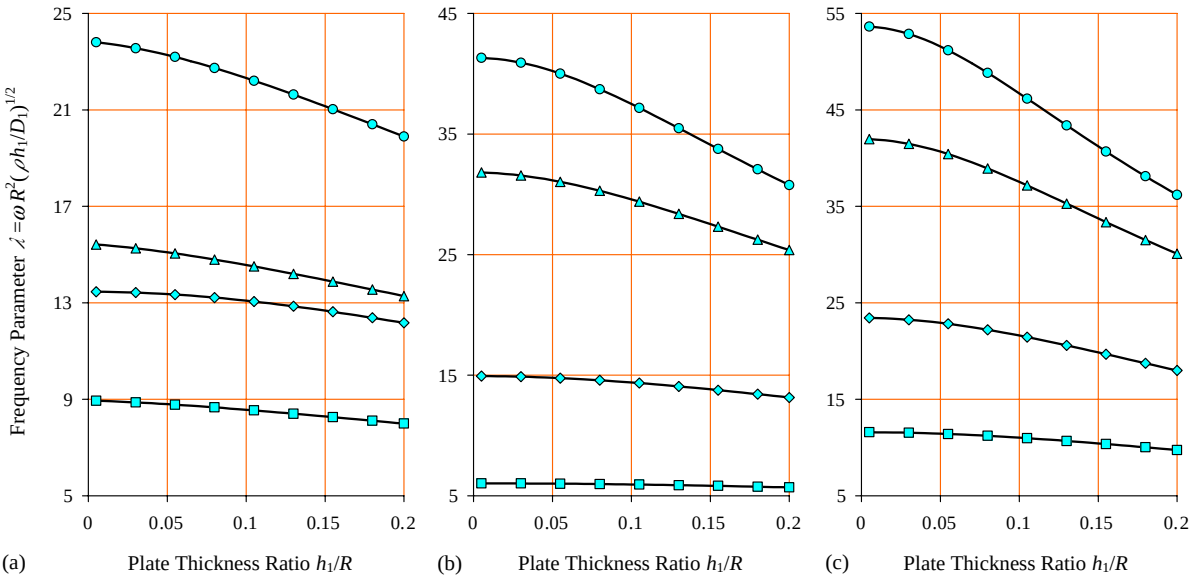

Fig. 6. Frequency parameters $\lambda = \omega R^2(\rho h_1/D_1)^{1/2}$ versus plate thickness ratio h_1/R for circular Mindlin plates (a) free, (b) simply supported, (c) clamped, having one step variation, step location ratio $r_2/R = 0.5$ and step thickness ratios $h_2/h_1 = 2$. □, First mode; ◇, second mode; △, third mode; and ○, fourth mode.

parameters with respect to the step location ratio r_2/R is more pronounced for free circular plates with smaller plate thickness ratio h_1/R. Figs. 3 and 4 show that the frequency parameters for simply supported and clamped circular plates increase monotonically as the step location ratio r_2/R changes from 0.01 to 0.99. Mode shape switching occurs for the simply supported and clamped circular Mindlin plates when the step location ratio r_2/R varies from 0.01 to 0.99 (see Figs. 3 and 4).

Fig. 5 shows the relationship between the first four frequency parameters λ and the step thickness ratio h_2/h_1 for free, simply supported and clamped circular Mindlin plates with one step variation. The step location ratio is fixed at $r_2/R = 0.5$ and the plate thickness ratio h_1/R is set to be 0.1, respectively. The curves in Fig. 5 start with the step thickness ratio $h_2/h_1 = 0.5$ and end with $h_2/h_1 = 2.5$ and there are 41 sample points on each curve. The frequency parameters λ for all cases in Fig. 5 increase monotonically as the step thickness ratio h_2/h_1 increases except for the second mode for the simply supported and the clamped plates and the first mode for the clamped plate. The frequency parameters λ of the second mode for the simply supported and the clamped plates increase initially as the step thickness ratio h_2/h_1 varies from 0.5 to 1.5 and then decrease when the step thickness ratio h_2/h_1 increases from 1.5 to 2.5. The frequency parameters λ of the first mode for the clamped plate decrease slightly and then increase as the step thickness ratio h_2/h_1 changes from 0.5 to 2.5. Mode shape switching is observed in the fourth mode for the free circular plate and in the third and fourth modes for the clamped plate as the step thickness ratio h_2/h_1 varies.

Fig. 6 presents the variation of the first four frequency parameters λ against the plate thickness ratio h_1/R for free, simply supported and clamped circular Mindlin plates with one step variation.

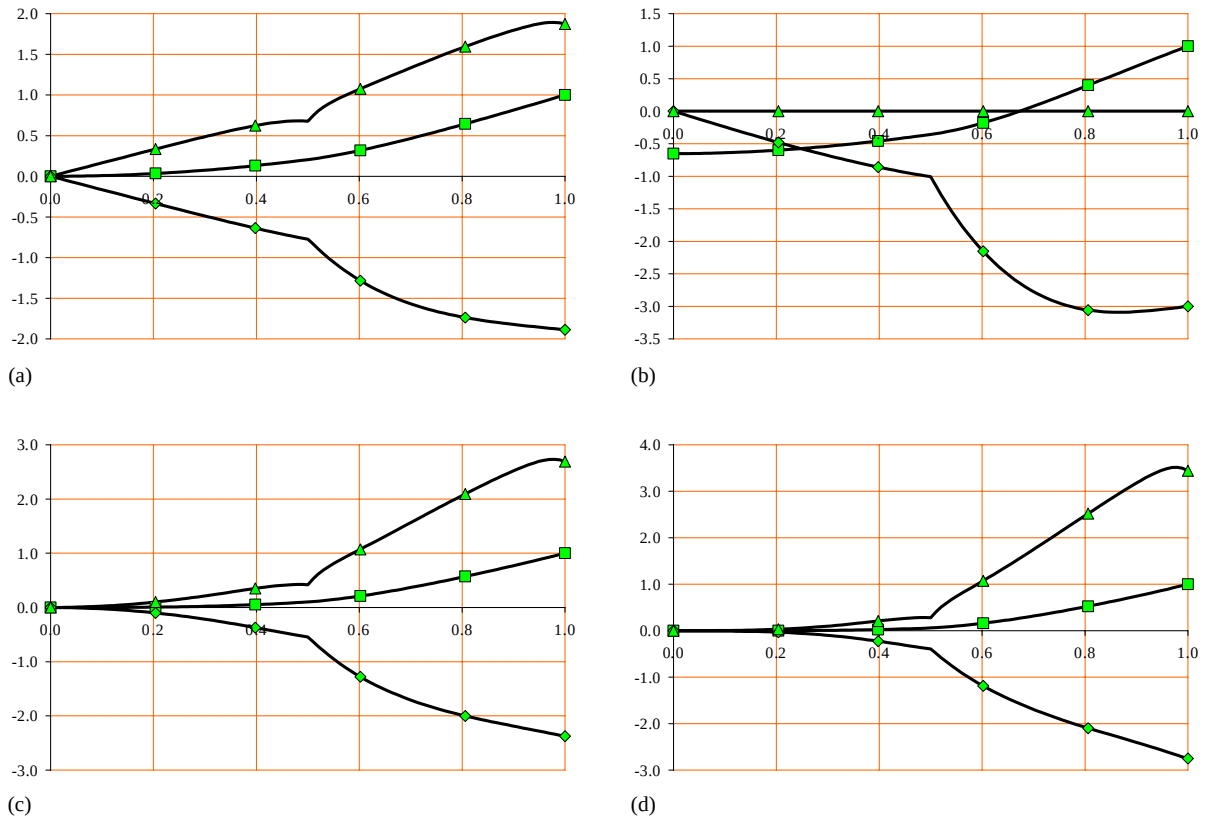

Fig. 7. Normalized modal shapes of displacement fields for free circular Mindlin plates with one step variation, plate thickness ratio $h_1/R = 0.1$, step location ratio $r_2/R = 0.5$ and step thickness ratios $h_2/h_1 = 2$. □, Transverse displacement $\bar{w}$; ◇, rotation ψ_r; and △, rotation ψ_θ. (a) First mode $(n, s) = (2, 1)$, (b) second mode $(n, s) = (0, 1)$, (c) third mode $(n, s) = (3, 1)$, (d) fourth mode $(n, s) = (0, 2)$.

The step location ratio is fixed at $r_2/R = 0.5$ and the step thickness ratio h_2/h_1 is set to be 2, respectively. The curves in Fig. 6 start with the plate thickness ratio $h_1/R = 0.005$ and end with $h_1/R = 0.2$ and there are 40 sample points on each curve. As expected, the frequency parameters λ decrease as the plate thickness ratio h_1/R increases. It is caused by the inclusion of the effect of transverse shear deformation and rotary inertia in the analysis. The decrease in rate of the frequency parameters λ is more pronounced if the plate is with a high edge constraint (in the order from free to simply supported to clamped) or the plate vibrates in higher modes.

Figs. 7–9 show the modal shapes of the displacement fields $\bar{w}$, ψ_r and ψ_θ for free, simply supported and clamped circular Mindlin plates with one step variation. The step location ratio, the step thickness ratio and the plate thickness ratio are set to be $r_2/R = 0.5$, $h_2/h_1 = 2$ and $h_1/R = 0.1$, respectively. The curves in Figs. 7–9 vary along the radial co-ordinate $\chi(= r/R)$ and there are 50 sample points on each curve. The modal shapes are normalized by multiplying the factor $|1/\bar{w}_{\max}|$. Although the step variation exists in the plates, the modal shapes for the

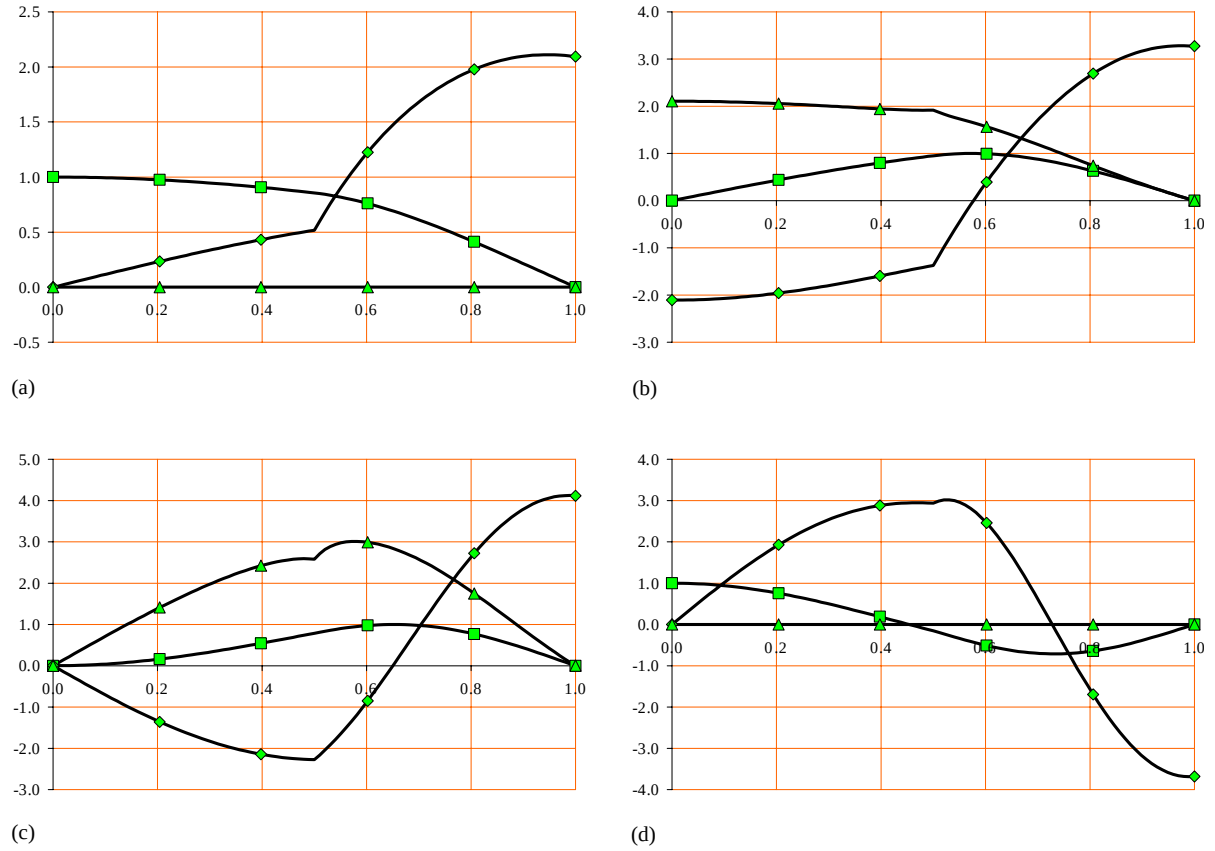

Fig. 8. Normalized modal shapes of displacement fields for simply supported circular Mindlin plates with one step variation, plate thickness ratio $h_1/R = 0.1$, step location ratio $r_2/R = 0.5$ and step thickness ratios $h_2/h_1 = 2$. □, Transverse displacement $\bar{w}$; ◇, rotation ψ_r; and △ rotation ψ_θ. (a) First mode $(n, s) = (0, 1)$, (b) second mode $(n, s) = (1, 1)$, (c) third mode $(n, s) = (2, 1)$, (d) fourth mode $(n, s) = (0, 2)$.

transverse displacement $\bar{w}$ for all cases are smooth at the location of step variation ($r_2/R = 0.5$). However, slope discontinuity at the location of step variation is observed for the modal shapes of rotations ψ_r and ψ_θ for all cases in Figs. 7–9 except for the cases with $n = 0$ (axisymmetric modes) where $\psi_\theta = 0$.

The influence of the step thickness ratio on the slope discontinuity of rotation ψ_r is further illustrated in Fig. 10 for a stepped simply supported circular Mindlin plate. The location of the step variation is at $r_2/R = 0.5$, the first step thickness to radius ratio is set to be $h_1/R = 0.005$, and the step thickness ratios are fixed at $h_2/h_1 = 1, 1.5, 2$ and 5, respectively. The modal shapes of rotation ψ_r are normalized so that the maximum positive value for each curve in Fig. 10 is equal to 1. There are 100 sample points on each curve in Fig. 10. It is observed that the level of the slope discontinuity in rotation ψ_r increases as the step thickness ratio h_2/h_1 becomes large. The slope discontinuity in the rotations is caused by the terms in Eqs. (4)–(10) through the terms τ_i and λ_i in Eq. (10) which are related to the step thickness.

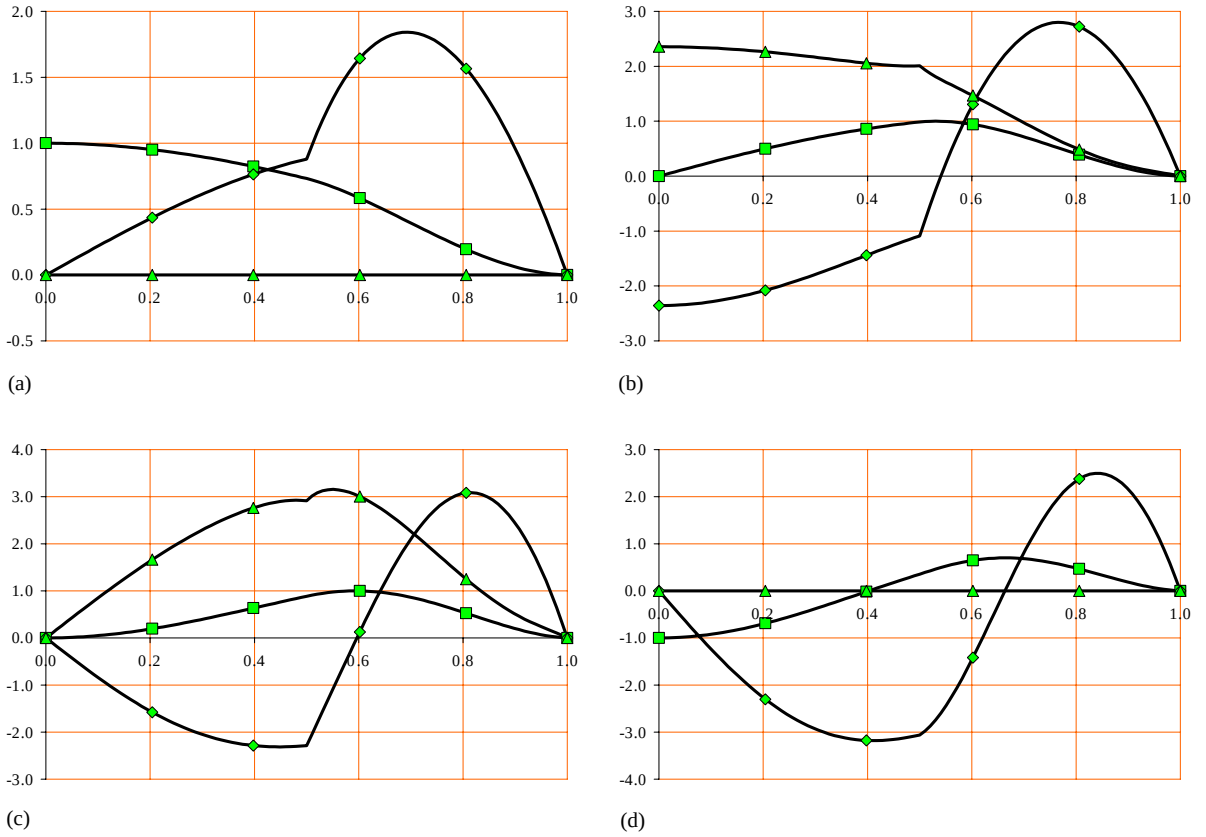

Fig. 9. Normalized modal shapes of displacement fields for clamped circular Mindlin plates with one step variation, plate thickness ratio $h_1/R = 0.1$, step location ratio $r_2/R = 0.5$ and step thickness ratios $h_2/h_1 = 2$. □, Transverse displacement $\bar{w}$; ◇, rotation ψ_i and △, rotation ψ_θ. (a) First mode $(n, s) = (0, 1)$, (b) second mode $(n, s) = (1, 1)$, (c) third mode $(n, s) = (2, 1)$, (d) fourth mode $(n, s) = (0, 2)$.

3.3. Circular plates with two step variations

Tables 5–8 present the exact frequency parameters λ of the first 10 modes for free, simply supported and clamped circular Mindlin plates with two step variations. The plate thickness ratio h_1/R is set to be 0.005 and 0.10 and the step location ratios are fixed at (1) $r_2/R = 0.5$ and $r_3/R = 0.1$, and (2) $r_2/R = 2/3$ and $r_3/R = 1/3$, respectively. Three sets of step thickness ratios are considered, i.e., (1) $h_2/h_1 = 1.5$ and $h_3/h_1 = 2.0$, (2) $h_2/h_1 = 2.0$ and $h_3/h_1 = 3.0$, and (3) $h_2/h_1 = 2/3$ and $h_3/h_1 = 1/3$. As for the plates with one step variation, the fundamental vibration mode for all simply supported and clamped plates in Tables 5–8 is axisymmetric ($n = 0$). The fundamental mode for all free plates is not axisymmetric, where two nodal diameters ($n = 2$) exist in the fundamental vibration mode. The frequency parameters λ decrease as the plate thickness ratio h_1/R increases due to the effect of transverse shear deformation and rotary inertia. On the other hand, the frequency parameters increase as the step thickness ratios h_2/h_1 and h_3/h_1 increase.

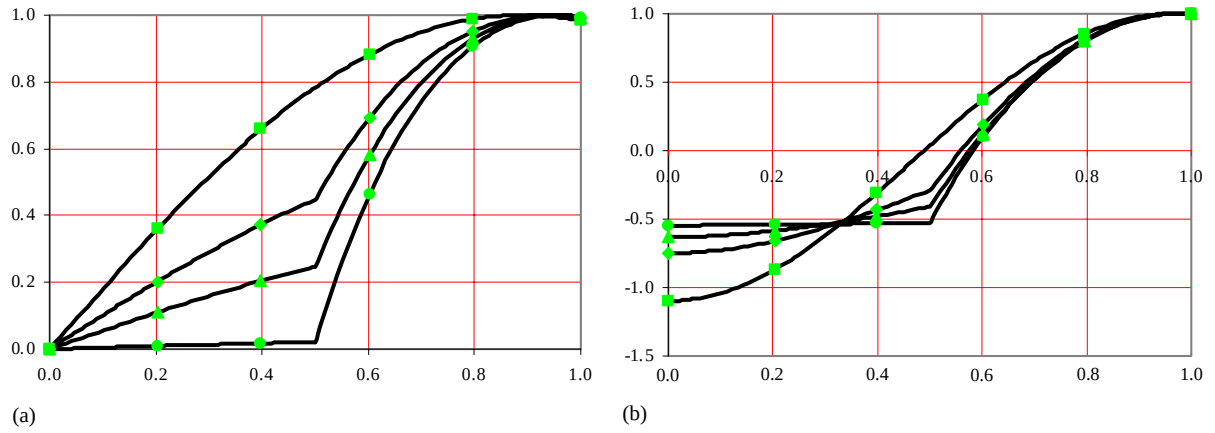

Fig. 10. Normalized modal shapes of displacement field ψ_r for simply supported circular Mindlin plates with one step variation, plate thickness ratio $h_1/R = 0.005$, step location ratio $r_2/R = 0.5$. □, $h_2/h_1 = 1$; ◇, $h_2/h_1 = 1.5$; △, $h_2/h_1 = 2$; and ○, $h_2/h_1 = 5$. (a) Mode (0,1), (b) mode (1,1).

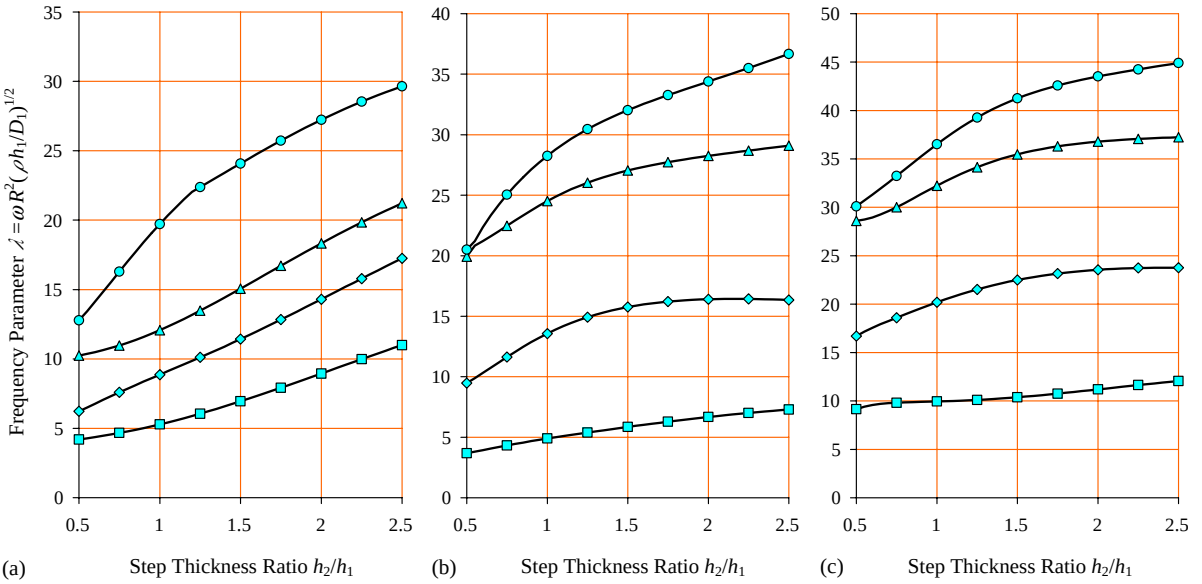

Fig. 11. Frequency parameters $\lambda = \omega R^2(\rho h_1/D_1)^{1/2}$ versus step thickness ratio h_2/h_1 for circular Mindlin plates (a) free, (b) simply supported, (c) clamped, having two step variations, step location ratios $r_3/R = 1/3$ and $r_2/R = 2/3$, step thickness ratios $h_3/h_1 = 1$, and plate thickness ratio $h_1/R = 0.1$. □, First mode; ◇, second mode; △, third mode; and ○, fourth mode.

Fig. 11 shows the variation of the first four frequency parameters λ versus the step thickness ratio h_2/h_1 for free, simply supported and clamped circular Mindlin plates with two step variations. The step location ratios are set to be $r_2/R = 2/3$ and $r_3/R = 1/3$, the plate thickness ratio is assumed to be $h_1/R = 0.1$ and the step thickness ratio h_3/h_1 is fixed at 1, respectively. The

Table 5
Frequency parameters $\lambda = \omega R^2\sqrt{\rho h_1/D_1}$ for circular Mindlin plates with two step variations ($h_1/R = 0.005, r_2/R = 0.5, r_3/R = 0.1$)

Boundary conditions	h_2/h_1	h_3/h_1	Mode sequence									
			1	2	3	4	5	6	7	8	9	10
Free	1.5	2.0	7.14706(2,1)	11.7618(0,1)	13.9348(3,1)	22.8595(4,1)	23.3539(1,1)	34.1194(5,1)	39.3782(2,2)	45.2273(0,2)	47.7163(6,1)	59.1107(3,2)
	2.0	3.0	9.11999(2,1)	13.5173(0,1)	15.4225(3,1)	23.8070(4,1)	24.0499(1,1)	34.6875(5,1)	43.0019(2,2)	48.0455(6,1)	52.4685(0,2)	63.7836(7,1)
	2/3	1/3	4.60648(2,1)	7.18332(0,1)	11.7586(3,1)	16.9077(1,1)	21.3197(4,1)	30.4896(0,2)	30.8551(2,2)	33.1350(5,1)	47.1262(6,1)	48.0888(3,2)
Simply supported	1.5	2.0	5.76982(0,1)	14.9432(1,1)	28.7439(2,1)	35.3983(0,2)	44.8075(3,1)	58.8269(1,2)	62.3016(4,1)	81.1282(5,1)	82.2146(2,2)	88.9525(0,3)
	2.0	3.0	6.02102(0,1)	14.9262(1,1)	32.4692(2,1)	41.8186(0,2)	50.6094(3,1)	65.7940(1,2)	67.9528(4,1)	85.6166(5,1)	87.7002(2,2)	96.3464(0,3)
	2/3	1/3	4.19133(0,1)	12.0765(1,1)	23.0997(2,1)	24.8516(0,2)	36.9645(3,1)	41.2427(1,2)	53.6381(4,1)	58.3687(0,3)	59.2281(2,2)	73.2291(5,1)
Clamped	1.5	2.0	11.1067(0,1)	23.2708(1,1)	38.9317(2,1)	46.8656(0,2)	57.3393(3,1)	74.0728(1,2)	77.4426(4,1)	98.3400(5,1)	101.464(2,2)	108.813(0,3)
	2.0	3.0	11.5708(0,1)	23.4358(1,1)	42.8272(2,1)	54.4135(0,2)	64.8062(3,1)	85.2691(1,2)	85.8598(4,1)	105.540(5,1)	109.998(2,2)	117.893(0,3)
	2/3	1/3	9.95141(0,1)	18.6792(1,1)	30.9058(2,1)	31.7770(0,2)	46.3795(3,1)	50.7446(1,2)	64.6016(4,1)	70.8071(2,2)	71.8506(0,3)	85.8306(5,1)

The values in brackets (n, s) denote the number of nodal diameters (n) and the mode sequence (s) for a given n value

Table 6
Frequency parameters $\lambda = \omega R^2\sqrt{\rho h_1/D_1}$ for circular Mindlin plates with two step variations ($h_1/R = 0.10$, $r_2/R = 0.5$, $r_3/R = 0.1$)

Boundary conditions	h_2/h_1	h_3/h_1	Mode sequence									
			1	2	3	4	5	6	7	8	9	10
Free	1.5	2.0	6.95711(2,1)	11.5033(0,1)	13.3905(3,1)	21.6542(4,1)	22.2578(1,1)	31.7725(5,1)	36.3708(2,2)	41.3770(0,2)	43.5479(6,1)	52.8238(3,2)
	2.0	3.0	8.69013(2,1)	13.1419(0,1)	14.5725(3,1)	22.3199(4,1)	22.7601(1,1)	32.1222(5,1)	38.9044(2,2)	43.7244(6,1)	46.4879(0,2)	56.8297(7,1)
	2/3	1/3	4.52221(2,1)	7.09854(0,1)	11.4022(3,1)	16.3069(1,1)	20.3326(4,1)	29.1154(2,2)	29.2482(0,2)	30.9851(5,1)	43.1106(6,1)	44.2926(3,2)
Simply supported	1.5	2.0	5.69927(0,1)	14.4894(1,1)	27.1614(2,1)	32.9289(0,2)	41.2097(3,1)	52.2968(1,2)	55.8058(4,1)	70.6314(2,2)	70.9304(5,1)	75.6162(0,3)
	2.0	3.0	5.93031(0,1)	14.3822(1,1)	29.9862(2,1)	37.8418(0,2)	45.1869(3,1)	56.8484(1,2)	59.2709(4,1)	73.4061(5,1)	73.5785(2,2)	79.4321(0,3)
	2/3	1/3	4.16532(0,1)	11.7902(1,1)	22.2052(2,1)	24.0043(0,2)	34.8276(3,1)	38.7684(1,2)	49.2816(4,1)	54.0713(0,3)	54.3267(2,2)	65.4045(5,1)
Clamped	1.5	2.0	10.6799(0,1)	21.7037(1,1)	35.3319(2,1)	41.9150(0,2)	50.4031(3,1)	62.7438(1,2)	65.7990(4,1)	81.1364(5,1)	82.0137(2,2)	86.9894(0,3)
	2.0	3.0	11.0049(0,1)	21.5861(1,1)	38.0416(2,1)	47.2086(0,2)	55.0772(3,1)	69.1703(1,2)	70.3441(4,1)	84.5376(5,1)	86.0533(2,2)	91.1101(0,3)
	2/3	1/3	9.74335(0,1)	17.8933(1,1)	28.9124(2,1)	30.0506(0,2)	42.2626(3,1)	46.2850(1,2)	57.1608(4,1)	62.6642(2,2)	63.7321(0,3)	73.5566(5,1)

The values in brackets (n, s) denote the number of nodal diameters (n) and the mode sequence (s) for a given n value

Table 7
Frequency parameters $\lambda = \omega R^2\sqrt{\rho h_1/D_1}$ for circular Mindlin plates with two step variations ($h_1/R = 0.005, r_2/R = 2/3, r_3/R = 1/3$)

Boundary conditions	h_2/h_1	h_3/h_1	Mode sequence									
			1	2	3	4	5	6	7	8	9	10
Free	1.5	2.0	8.91754(2,1)	14.7470(0,1)	16.5157(3,1)	25.9224(4,1)	28.5529(1,1)	37.3040(5,1)	46.1109(2,2)	50.7413(6,1)	53.0158(0,2)	65.5614(3,2)
	2.0	3.0	13.2056(2,1)	19.9394(0,1)	21.2110(3,1)	30.3192(4,1)	33.3980(1,1)	41.1128(5,1)	52.1937(2,2)	53.9034(6,1)	61.8251(0,2)	68.8698(7,1)
	2/3	1/3	4.02776(2,1)	6.01948(0,1)	10.7570(3,1)	13.5151(1,1)	19.9920(4,1)	23.9130(0,2)	25.7083(2,2)	31.6243(5,1)	37.2194(1,2)	41.0072(3,2)
Simply supported	1.5	2.0	6.73089(0,1)	17.0342(1,1)	31.8611(2,1)	39.8132(0,2)	48.4109(3,1)	64.5688(1,2)	67.5753(4,1)	89.3114(5,1)	94.6366(2,2)	104.443(0,3)
	2.0	3.0	7.64222(0,1)	17.9206(1,1)	36.6646(2,1)	48.2960(0,2)	56.4333(3,1)	79.1014(4,1)	79.7602(1,2)	103.815(5,1)	117.623(2,2)	129.018(6,1)
	2/3	1/3	3.69122(0,1)	10.1010(1,1)	19.9762(2,1)	20.1062(0,2)	31.3902(1,2)	32.6611(3,1)	41.8707(0,3)	47.3229(2,2)	48.1669(4,1)	63.6252(1,3)
Clamped	1.5	2.0	11.8787(0,1)	26.0122(1,1)	43.8340(2,1)	53.4371(0,2)	62.5817(3,1)	80.5902(1,2)	83.6487(4,1)	107.679(5,1)	112.634(2,2)	122.854(0,3)
	2.0	3.0	13.3744(0,1)	28.2892(1,1)	49.4568(2,1)	62.5284(0,2)	71.1687(3,1)	96.3650(4,1)	96.5483(1,2)	125.036(5,1)	140.359(2,2)	155.113(6,1)
	2/3	1/3	9.80761(0,1)	16.5495(1,1)	26.5570(0,2)	27.0936(2,1)	39.4257(1,2)	40.5358(3,1)	49.1955(0,3)	55.5653(2,2)	57.0479(4,1)	70.4269(1,3)

The values in brackets (n, s) denote the number of nodal diameters (n) and the mode sequence (s) for a given n value

Table 8
Frequency parameters $\lambda = \omega R^2\sqrt{\rho h_1/D_1}$ for circular Mindlin plates with two step variations ($h_1/R = 0.10, r_2/R = 2/3, r_3/R = 1/3$)

Boundary conditions	h_2/h_1	h_3/h_1	Mode sequence									
			1	2	3	4	5	6	7	8	9	10
Free	1.5	2.0	8.64131(2,1)	14.2970(0,1)	15.7309(3,1)	24.2700(4,1)	26.7991(1,1)	34.2976(5,1)	41.7196(2,2)	45.7580(6,1)	47.3391(0,2)	57.3719(3,2)
	2.0	3.0	12.4084(2,1)	18.9759(0,1)	19.5384(3,1)	27.5316(4,1)	30.7345(1,1)	36.8559(5,1)	45.9272(2,2)	47.6712(6,1)	52.9887(0,2)	59.9520(7,1)
	2/3	1/3	3.94684(2,1)	5.96010(0,1)	10.4301(3,1)	13.0014(1,1)	19.0926(4,1)	23.2801(0,2)	24.3579(2,2)	29.6403(5,1)	35.3855(1,2)	38.1428(3,2)
Simply supported	1.5	2.0	6.61467(0,1)	16.3417(1,1)	29.7116(2,1)	36.4009(0,2)	43.9133(3,1)	56.3120(1,2)	59.5587(4,1)	76.3619(5,1)	78.4203(2,2)	84.5269(0,3)
	2.0	3.0	7.44372(0,1)	16.9413(1,1)	33.1898(2,1)	42.3607(0,2)	49.1513(3,1)	65.2431(1,2)	66.3787(4,1)	84.1066(5,1)	90.0304(2,2)	97.0542(0,3)
	2/3	1/3	3.67234(0,1)	9.84061(1,1)	19.2783(2,1)	19.6735(0,2)	30.0635(1,2)	31.0172(3,1)	40.1603(0,3)	44.3326(2,2)	44.8090(4,1)	59.7072(1,3)
Clamped	1.5	2.0	11.3152(0,1)	23.7479(1,1)	38.6283(2,1)	46.1750(0,2)	53.5294(3,1)	66.5535(1,2)	69.5023(4,1)	86.6246(5,1)	88.6546(2,2)	94.7115(0,3)
	2.0	3.0	12.4167(0,1)	24.9392(1,1)	42.0639(2,1)	51.7205(0,2)	58.5030(3,1)	74.9068(1,2)	76.3120(4,1)	94.9219(5,1)	100.897(2,2)	108.413(0,3)
	2/3	1/3	9.64461(0,1)	15.9370(1,1)	25.5801(0,2)	25.6633(2,1)	36.9919(1,2)	37.6163(3,1)	46.1207(0,3)	50.8187(2,2)	51.6433(4,1)	65.0309(1,3)

The values in brackets (n, s) denote the number of nodal diameters (n) and the mode sequence (s) for a given n value

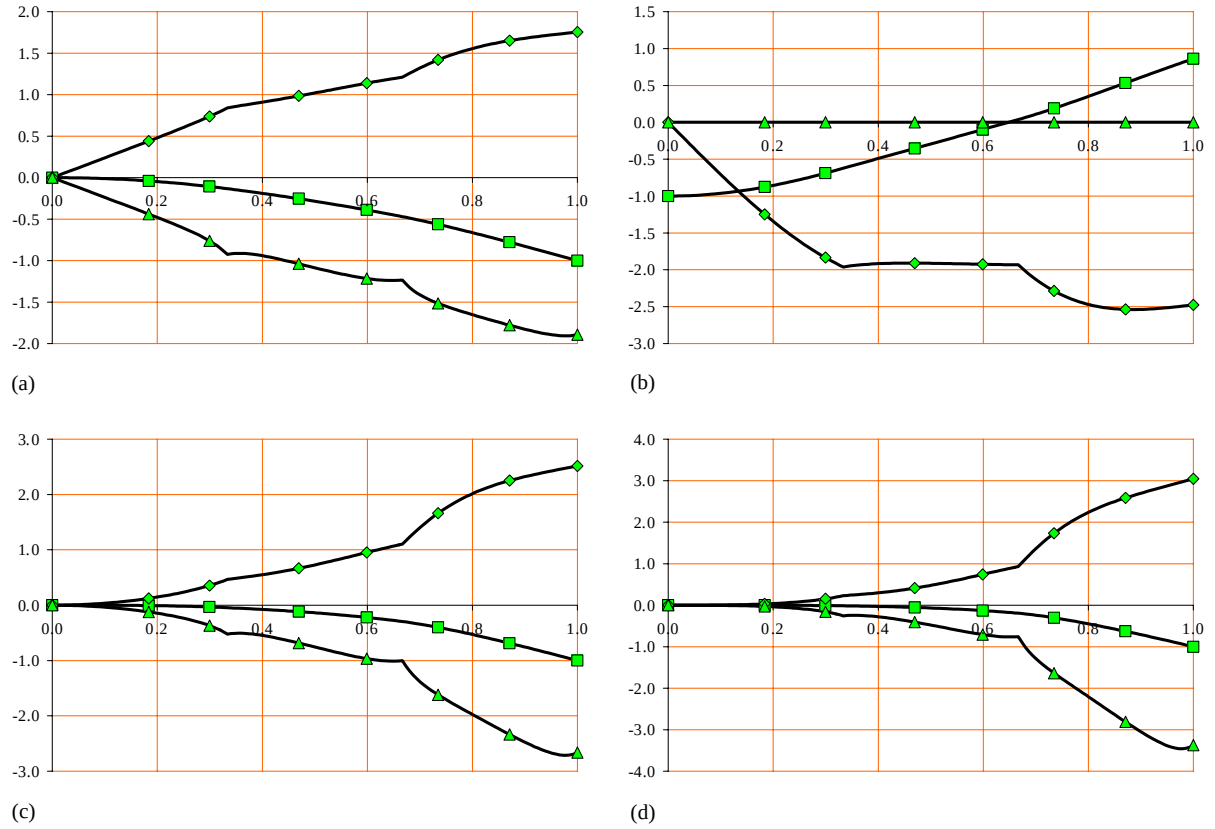

Fig. 12. Normalized modal shapes of displacement fields for free circular Mindlin plates with two step variations, plate thickness ratio $h_1/R = 0.1$, step location ratios $r_3/R = 1/3$ and $r_2/R = 2/3$ and step thickness ratios $h_3/h_1 = 1$ and $h_2/h_1 = 2$. □, Transverse displacement $\bar{w}$; ◇, rotation ψ_r; and △ rotation ψ_θ. (a) First mode, $\lambda = 8.94859, (n, s) = (2, 1)$; (b) second mode, $\lambda = 14.3028, (n, s) = (0, 1)$; (c) third mode, $\lambda = 18.3323, (n, s) = (3, 1)$; (d) fourth mode, $\lambda = 27.2307, (n, s) = (4, 1)$.

step thickness ratio of the middle step to the outer step h_2/h_1 varies from 0.5 to 2.5 and there are 41 sample points on each curve in Fig. 11. It is observed that the frequency parameters λ for all cases in Fig. 10 increase monotonically as the step thickness ratio h_2/h_1 increases. Mode shape switching is observed in the third and fourth modes for the simply supported circular plate near the location of $h_2/h_1 \approx 0.6$.

Fig. 12 shows the modal shapes of the displacement fields $\bar{w}$, ψ_r and ψ_θ for free circular Mindlin plates with two step variations. The step location ratios are set to be $r_2/R = 2/3$ and $r_3/R = 1/3$, the plate thickness ratio is assumed to be $h_1/R = 0.1$ and the step thickness ratios are fixed at $h_2/h_1 = 2$ and $h_3/h_1 = 1$, respectively. The curves in Fig. 12 vary along the radial co-ordinate $\chi(= r/R)$ and there are 50 sample points on each curve. The modal shapes are normalized by multiplying the factor $|1/\bar{w}_{\max}|$. Slope discontinuity at the location of the two step variations is observed for the modal shapes of rotations ψ_r and ψ_θ for the first four modes of the free circular plate except for the rotation ψ_θ of the second mode where $\psi_\theta = 0$ (axisymmetric mode).

Table 9
Frequency parameters $\lambda = \omega R^2\sqrt{\rho h_1/D_1}$ for circular Mindlin plates with three step variations ($h_1/R = 0.10, r_2/R = 0.75, r_3/R = 0.5, r_4/R = 0.1$)

Boundary conditions	h_2/h_1	h_3/h_1	h_4/h_1	Mode sequence									
				1	2	3	4	5	6	7	8	9	10
Free	2.0	3.0	4.0	15.2993(2,1)	24.0114(0,1)	24.6202(3,1)	33.6264(4,1)	38.9717(1,1)	43.3299(5,1)	54.0918(6,1)	54.2915(2,2)	61.3592(0,2)	66.0136(7,1)
	3/4	2/4	1/4	3.80464(2,1)	5.75676(0,1)	10.0299(3,1)	12.9074(1,1)	18.4406(4,1)	22.3227(0,2)	23.5735(2,2)	28.7651(5,1)	36.4306(1,2)	36.7675(3,2)
Simply supported	2.0	3.0	4.0	8.86487(0,1)	19.5754(1,1)	36.1958(2,1)	46.3641(0,2)	53.7009(3,1)	71.4386(1,2)	71.5331(4,1)	89.8558(5,1)	95.3708(2,2)	102.290(0,3)
	3/4	2/4	1/4	3.57232(0,1)	9.72302(1,1)	18.7136(0,2)	18.7633(2,1)	30.0318(3,1)	31.2022(1,2)	43.1485(4,1)	44.5371(0,3)	44.6863(2,2)	58.0201(5,1)
Clamped	2.0	3.0	4.0	13.5857(0,1)	27.6263(1,1)	45.2373(2,1)	55.7032(0,2)	63.4342(3,1)	81.1374(1,2)	81.6425(4,1)	100.152(5,1)	104.974(2,2)	111.586(0,3)
	3/4	2/4	1/4	9.22339(0,1)	16.2366(1,1)	25.3761(2,1)	25.4378(0,2)	36.8511(3,1)	38.5416(1,2)	50.0245(4,1)	52.4728(2,2)	53.3446(0,3)	64.8946(5,1)

The values in brackets (n, s) denote the number of nodal diameters (n) and the mode sequence (s) for a given n value

Table 10
Frequency parameters $\lambda = \omega R^2\sqrt{\rho h_1/D_1}$ for circular Mindlin plates with three step variations ($h_1/R = 0.10, r_2/R = 3/4, r_3/R = 2/4, r_4/R = 1/4$)

Boundary conditions	h_2/h_1	h_3/h_1	h_4/h_1	Mode sequence									
				1	2	3	4	5	6	7	8	9	10
Free	2.0	3.0	4.0	16.3103(2,1)	24.7868(0,1)	24.8291(3,1)	33.6542(4,1)	38.9810(1,1)	43.3331(5,1)	54.0921(6,1)	55.4994(2,2)	62.9871(0,2)	66.0137(7,1)
	3/4	2/4	1/4	3.75557(2,1)	5.60669(0,1)	10.0088(3,1)	12.1957(1,1)	18.4342(4,1)	22.0338(0,2)	22.9023(2,2)	28.7635(5,1)	32.6403(1,2)	36.0984(3,2)
Simply supported	2.0	3.0	4.0	8.87155(0,1)	19.4849(1,1)	37.6984(2,1)	48.1586(0,2)	54.2815(3,1)	71.6630(4,1)	71.9623(1,2)	89.8795(5,1)	96.8984(2,2)	104.264(0,3)
	3/4	2/4	1/4	3.50279(0,1)	9.34591(1,1)	18.3545(2,1)	18.6948(0,2)	28.1214(1,2)	29.6625(3,1)	39.4829(0,3)	41.9982(2,2)	42.9671(4,1)	54.6951(1,3)
Clamped	2.0	3.0	4.0	13.6439(0,1)	27.4930(1,1)	46.8578(2,1)	57.7372(0,2)	64.1404(3,1)	81.8117(4,1)	81.8929(1,2)	100.184(5,1)	106.455(2,2)	113.503(0,3)
	3/4	2/4	1/4	9.43807(0,1)	15.3630(1,1)	24.6242(2,1)	24.7508(0,2)	34.7282(1,2)	36.1785(3,1)	45.6142(0,3)	48.8310(2,2)	49.6854(4,1)	62.5342(1,3)

The values in brackets (n, s) denote the number of nodal diameters (n) and the mode sequence (s) for a given n value

Table 11
Frequency parameters $\lambda = \omega R^2\sqrt{\rho h_1/D_1}$ for circular Mindlin plates with four step variations ($h_1/R = 0.10, r_2/R = 0.75, r_3/R = 0.5, r_4/R = 0.25, r_5/R = 0.1$)

Boundary conditions	h_2/h_1	h_3/h_1	h_4/h_1	h_5/h_1	Mode sequence									
					1	2	3	4	5	6	7	8	9	10
Free	2.0	3.0	4.0	5.0	16.4688(2,1)	24.8334(3,1)	24.8442(0,1)	33.6543(4,1)	38.9425(1,1)	43.3331(5,1)	54.0921(6,1)	55.7520(2,2)	63.1143(0,2)	66.0137(7,1)
	4/5	3/5	2/5	1/5	3.95427(2,1)	5.96600(0,1)	10.3291(3,1)	13.7692(1,1)	18.8330(4,1)	25.0059(2,2)	25.0273(0,2)	29.2074(5,1)	37.5346(1,2)	38.8270(3,2)
Simply supported	2.0	3.0	4.0	5.0	8.85637(0,1)	19.4579(1,1)	37.9726(2,1)	48.3078(0,2)	54.2947(3,1)	71.6635(4,1)	71.8825(1,2)	89.8795(5,1)	97.3193(2,2)	104.254(0,3)
	4/5	3/5	2/5	1/5	3.65755(0,1)	10.3023(1,1)	19.6398(2,1)	20.6401(0,2)	31.3722(3,1)	31.9806(1,2)	44.9775(4,1)	46.9782(2,2)	47.0348(0,3)	60.1748(5,1)
Clamped	2.0	3.0	4.0	5.0	13.6221(0,1)	27.4461(1,1)	47.1722(2,1)	57.9121(0,2)	64.1570(3,1)	81.8123(4,1)	81.8223(1,2)	100.184(5,1)	106.882(2,2)	113.407(0,3)
	4/5	3/5	2/5	1/5	9.35984(0,1)	16.5228(1,1)	26.3165(2,1)	27.4721(0,2)	38.4450(3,1)	39.1365(1,2)	52.3004(4,1)	54.6448(2,2)	54.8976(0,3)	67.6033(5,1)

The values in brackets (n, s) denote the number of nodal diameters (n) and the mode sequence (s) for a given n value

Table 12
Frequency parameters $\lambda = \omega R^2\sqrt{\rho h_1/D_1}$ for circular Mindlin plates with four step variations ($h_1/R = 0.10, r_2/R = 4/5, r_3/R = 3/5, r_4/R = 2/5, r_5/R = 1/5$)

Boundary conditions	h_2/h_1	h_3/h_1	h_4/h_1	h_5/h_1	Mode sequence									
					1	2	3	4	5	6	7	8	9	10
Free	2.0	3.0	4.0	5.0	20.0942(2,1)	30.0692(3,1)	30.2317(0,1)	39.9295(4,1)	46.7406(1,1)	50.2774(5,1)	61.3739(6,1)	64.7768(2,2)	72.5784(0,2)	73.3507(7,1)
	4/5	3/5	2/5	1/5	3.64134(2,1)	5.40621(0,1)	9.74772(3,1)	11.7113(1,1)	18.0102(4,1)	21.2039(0,2)	22.0424(2,2)	28.1752(5,1)	31.1995(1,2)	34.8522(3,2)
Simply supported	2.0	3.0	4.0	5.0	10.1902(0,1)	21.7838(1,1)	42.0050(2,1)	53.5103(0,2)	59.4745(3,1)	77.3177(4,1)	78.4329(1,2)	95.7491(5,1)	103.592(2,2)	110.746(0,3)
	4/5	3/5	2/5	1/5	3.40191(0,1)	9.03774(1,1)	17.7890(2,1)	18.0754(0,2)	27.0194(1,2)	28.8119(3,1)	38.4211(0,3)	40.3668(2,2)	41.8189(4,1)	51.5030(1,3)
Clamped	2.0	3.0	4.0	5.0	14.7395(0,1)	29.4786(1,1)	50.8330(2,1)	62.6341(0,2)	69.1664(3,1)	87.4270(4,1)	88.1236(1,2)	105.991(5,1)	112.948(2,2)	119.737(0,3)
	4/5	3/5	2/5	1/5	9.30274(0,1)	14.9738(1,1)	23.9515(2,1)	24.0653(0,2)	33.5078(1,2)	35.2395(3,1)	45.0182(0,3)	47.2332(2,2)	48.4542(4,1)	58.9996(1,3)

The values in brackets (n, s) denote the number of nodal diameters (n) and the mode sequence (s) for a given n value

3.4. Circular plates with three and four step variations

Tables 9–12 present the exact frequency parameters λ of the first 10 modes for free, simply supported and clamped circular Mindlin plates with three and four step variations. The plate thickness ratio h_1/R is set to be 0.1. For plates with three step variations, the locations of the step variations are at (1) $r_2/R = 0.75$, $r_3/R = 0.5$, $r_4/R = 0.1$ and (2) $r_2/R = 3/4$, $r_3/R = 2/4$, $r_4/R = 1/4$, and two sets of step thickness ratios $(h_2/h_1,\ h_3/h_1,\ h_4/h_1) = (2, 3, 4; 3/4, 2/4, 1/4)$ are considered. For plates with four step variations, the locations of the step variations are at (1) $r_2/R = 0.75$, $r_3/R = 0.5$, $r_4/R = 0.25$ and $r_5/R = 0.1$ and (2) $r_2/R = 4/5$, $r_3/R = 3/5$, $r_4/R = 2/5$ and $r_5/R = 1/5$, and two sets of step thickness ratios $(h_2/h_1,\ h_3/h_1,\ h_4/h_1,\ h_5/h_1) = (2, 3, 4, 5; 4/5, 3/5, 2/5, 1/5)$ are considered. The fundamental vibration modes for plates in Tables 9–12 show the same trends as for the plates with one and two step variations.

4. Conclusions

This paper presents an investigation on the vibration behaviour of circular Mindlin plates with step-wise thickness variations. First-known exact vibration frequencies for stepped circular Mindlin plates are obtained. The influence of the plate thickness ratios, the step thickness ratios and the locations of the step variations on the frequency parameters are examined. The exact vibration solutions may serve as benchmark values for researchers to check the validity and accuracy of their numerical methods for such plate vibration problems.

Acknowledgements

The work described in this paper was fully supported by a research grant from the University of Western Sydney (Grand No. 20801-80355).

References

[1] A.W. Leissa, *Vibration of Plates*, NASA SP-169, Office of Technology Utilization, NASA, Washington, DC, 1969. Reprinted by The Acoustical Society of America, 1993.
[2] A.W. Leissa, Recent research in plate vibrations: classical theory, *Shock and Vibration Digest* 9 (1977) 13–24.
[3] A.W. Leissa, Recent research in plate vibrations: complicating effects, *Shock and Vibration Digest* 9 (1977) 21–35.
[4] A.W. Leissa, Plate vibration research, 1976–1980: classical theory, *Shock and Vibration Digest* 13 (1981) 11–22.
[5] A.W. Leissa, Plate vibration research, 1976–1980: complicating effects, *Shock and Vibration Digest* 13 (1981) 19–36.
[6] A.W. Leissa, Recent research in plate vibrations, 1981–1985, Part I. Classical theory, *Shock and Vibration Digest* 19 (1987) 11–18.
[7] A.W. Leissa, Recent research in plate vibrations, 1981–1985, Part II. Complicating effects, *Shock and Vibration Digest* 19 (1987) 10–24.
[8] J.H. Kang, A.W. Leissa, Three-dimensional vibrations of thick, linearly tapered, annular plates, *Journal of Sound and Vibration* 217 (1998) 927–944.
[9] U.S. Gupta, A.H. Ansari, Free vibration of polar orthotropic circular plates of variable thickness with elastically restrained edge, *Journal of Sound and Vibration* 213 (1998) 429–445.

[10] U.S. Gupta, A.H. Ansari, Asymmetric vibrations and elastic stability of polar orthotropic circular plates of linearly varying profile, *Journal of Sound and Vibration* 215 (1998) 231–250.
[11] H.P. Lee, T.Y. Ng, Vibration and critical speeds of a spinning annular disk of varying thickness, *Journal of Sound and Vibration* 187 (1995) 39–50.
[12] J. Wang, Generalized power series solutions of the vibration of classical circular plates with variable thickness, *Journal of Sound and Vibration* 202 (1997) 593–599.
[13] D.Y. Chen, B.S. Ren, Finite element analysis of the lateral vibration of thin annular and circular plates with variable thickness, *American Society of Mechanical Engineers, Journal of Vibration and Acoustics* 120 (1998) 747–752.
[14] B. Singh, S.M. Hassan, Transverse vibration of a circular plate with arbitrary thickness variation, *International Journal of Mechanical Sciences* 40 (1998) 1089–1104.
[15] A.P. Gupta, N. Sharma, Forced axisymmetric response of an annular plate of parabolically varying thickness, *International Journal of Mechanical Sciences* 41 (1999) 71–83.
[16] Z.M. Ye, Application of Maple V to the nonlinear vibration analysis of circular plate with variable thickness, *Computers and Structures* 71 (1999) 481–488.
[17] T.Y. Wu, G.R. Liu, Free vibration analysis of circular plates with variable thickness by the generalized differential quadrature rule, *International Journal of Solids and Structures* 38 (2001) 7967–7980.
[18] A. Gajewski, Vibration and stability of annular plates in non-linear creep conditions, *Journal of Sound and Vibration* 249 (2002) 447–463.
[19] T. Irie, G. Yamada, S. Aomura, Free vibrations of a Mindlin annular plate of varying thickness, *Journal of Sound and Vibration* 66 (1979) 187–197.
[20] L.E. Luisoni, P.A.A. Laura, R. Grossi, Antisymmetric modes of vibration of circular plate elastically restrained against rotation and of linearly varying thickness, *Journal of Sound and Vibration* 54 (1977) 62–66.
[21] P.A.A. Laura, R.H. Gutierrez, Analysis of vibration circular plates of non-uniform thickness by the method of differential quadrature, *Ocean Engineering* 22 (1995) 97–100.
[22] A.P. Gupta, N. Goyal, Forced asymmetric response of linearly tapered circular plates, *Journal of Sound and Vibration* 220 (1999) 641–657.
[23] U.S. Gupta, A.H. Ansari, Effect of elastic foundation on asymmetric vibration of polar orthotropic linearly tapered circular plates, *Journal of Sound and Vibration* 254 (2002) 411–426.
[24] J. Wang, Free vibration of stepped circular plates on elastic foundations, *Journal of Sound and Vibration* 159 (1992) 175–181.
[25] R.D. Avalos, P.A.A. Laura, H. Larrondo, Transverse vibrations and buckling of circular plates of discontinuously varying thickness subject to and in-plane state of hydrostatic stress, *Ocean Engineering* 22 (1995) 105–110.
[26] F. Ju, H.P. Lee, K.H. Lee, Free vibration of plates with stepped variation in thickness on non-homogeneous elastic foundations, *Journal of Sound and Vibration* 183 (1995) 533–545.
[27] D.R. Avalos, H.A. Larrondo, V. Sonzogni, P.A.A. Laura, A general approximate solution of the problem of free vibrations of annular plates of stepped thickness, *Journal of Sound and Vibration* 196 (1996) 275–283.
[28] H.Z. Gu, X.W. Wang, On the free vibration analysis of circular plates with stepped thickness over a concentric region by the differential quadrature element method, *Journal of Sound and Vibration* 202 (1997) 452–459.
[29] Y. Xiang, Exact vibration solutions for circular Mindlin plates with multiple concentric ring supports, *International Journal of Solids and Structures* 39 (2002) 6081–6102.
[30] R.D. Mindlin, Influence of rotatory inertia and shear on flexural motions of isotropic, elastic plates, *American Society of Mechanical Engineers, Journal of Applied Mechanics* 18 (1951) 31–38.
[31] R.D. Mindlin, H. Deresiewicz, Thickness-shear and flexural vibrations of a circular disk, *Journal of Applied Physics* 25 (1954) 1329–1332.
[32] H. Deresiewicz, R.D. Mindlin, Axially symmetric flexural vibration of a circular disk, *American Society of Mechanical Engineers, Journal of Applied Mechanics* 22 (1955) 86–88.
[33] K.M. Liew, C.M. Wang, Y. Xiang, S. Kitipornchai, *Vibration of Mindlin Plates—Programming the p-Version Ritz Method*, Elsevier, Oxford, UK, 1988.